

Article

Temperature Characterization of Unipolar-Doped Electroluminescence in Vertical GaN/AlN Heterostructures

Weidong Zhang ^{1,*}, Tyler A. Growden ^{2,3,†}, Paul R. Berger ³ , David F. Storm ², David J. Meyer ² and Elliott R. Brown ^{1,*}

¹ Departments of Physics and Electrical Engineering, Wright State University, Dayton, OH 45435, USA;

² U.S. Naval Research Laboratory, Washington, DC 20375, USA; tag5050@gmail.com (T.A.G.); david.storm@nrl.navy.mil (D.F.S.); david.meyer@nrl.navy.mil (D.J.M.)

³ Department of Electrical and Computer Engineering, The Ohio State University, Columbus, OH 43210, USA; pberger@ieee.org

* Correspondence: wzzhang@fastmail.fm (W-D.Z.); elliot.brown@wright.edu (E.R.B.)

† These authors contributed equally to this work.

Abstract: An electroluminescence (EL) phenomenon in unipolar-doped GaN/AlN/GaN double-barrier heterostructures—without any p-type contacts—was investigated from 4.2 K to 300 K. In the range of 200–300 K, the extracted peak photon energies agree with the Monemar formula. In the range of 30 to 200 K, the photon energies are consistent with A-exciton emission. At 4.2 K, the exciton type likely transforms into B-exciton. These studies confirm that the EL emission comes from a cross-bandgap (or band-to-band) electron-hole radiative recombination and is excitonic. The excitons are formed by the holes generated through interband tunneling and the electrons injected into the GaN emitter region of the GaN/AlN heterostructure devices.

Keywords: GaN/AlN; electroluminescence; unipolar; holes; interband tunneling; exciton emission; A exciton; B exciton



Citation: Zhang, W.; Growden, T.A.; Berger, P.R.; Storm, D.F.; Meyer, D.J.; Brown, E.R. Temperature Characterization of Unipolar-Doped Electroluminescence in Vertical GaN/AlN Heterostructures. *Energies* **2021**, *14*, 6654. <https://doi.org/10.3390/en14206654>

Academic Editors: Gregorio García and Alexey A. Sokol

Received: 20 August 2021

Accepted: 7 October 2021

Published: 14 October 2021

Publisher's Note: MDPI stays neutral with regard to jurisdictional claims in published maps and institutional affiliations.



Copyright: © 2021 by the authors. Licensee MDPI, Basel, Switzerland. This article is an open access article distributed under the terms and conditions of the Creative Commons Attribution (CC BY) license (<https://creativecommons.org/licenses/by/4.0/>).

1. Introduction

In GaN-based LEDs and laser diodes, two types of contacts are required for generating light emission. One is n-type, which acts as reservoir for electrons; the other is p-type, which acts as reservoir for holes. However, there are a few exceptions. Recently, we reported an electroluminescence (EL) phenomenon observed in unipolar n-doped GaN/AlN/GaN double-barrier resonant tunneling diodes (RTDs) without any p-type contacts (Figure 1a–c) [1]. We hypothesized that the holes necessary for the EL are generated near the depleted spacer region on the collector side of GaN/AlN RTDs via Zener interband tunneling, which is enabled by the unusually high electric fields—on the order of $\sim 5 \times 10^6$ V/cm—originating from the polarization effect that is native to Wurtzite heterostructures (Figure 1d) [2]. The holes migrate to the emitter region, where they can radiatively recombine with those electrons injected from the emitter contact (Figure 1d). Hence, the emission is a cross-bandgap recombination. This is supported by the fact that the peak wavelength of the emission is ~ 360 nm with photon energy equal to the bandgap of GaN at room temperature (~ 3.44 eV) [3] (Figure 1b).

In this letter, we report temperature dependent studies on the unipolar EL in n-doped GaN/AlN heterostructures. The results not only further verify that the EL is a cross-bandgap (or band-to-band) radiative recombination, but also reveal its excitonic nature.

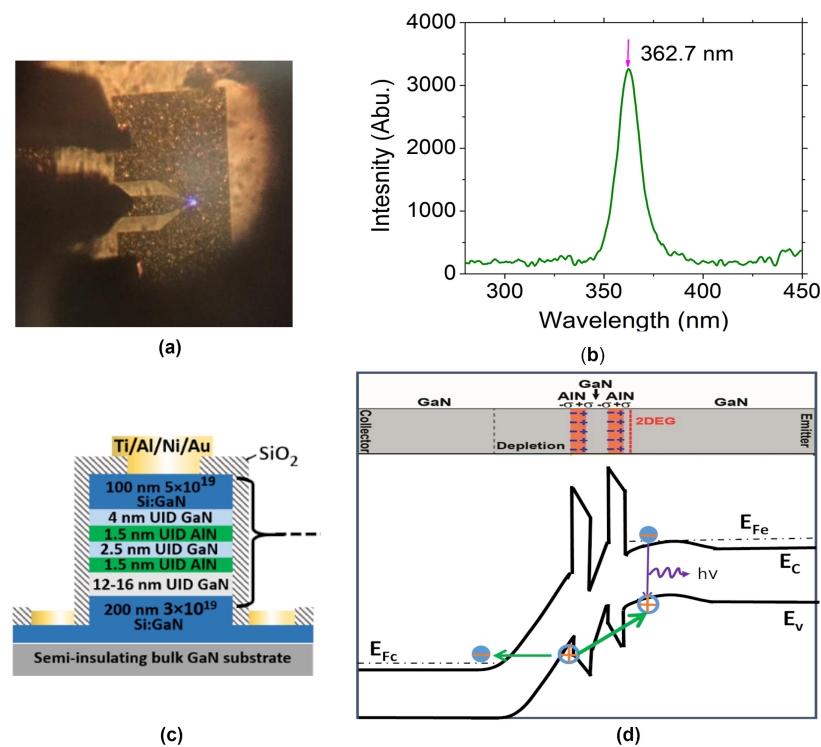


Figure 1. (a) Unipolar near-UV EL. (b) Spectrum of the EL emission. (c) Structure of GaN/AlN/GaN heterostructure stack. (d) An illustration of the hole generation process and the cross-bandgap optical recombination.

2. Materials and Methods

The GaN/AlN double-barrier heterostructures were grown via plasma-assisted molecular-beam epitaxy (PAMBE) at 860 °C on free standing Ga-polar semi-insulating GaN substrates created separately using hydride vapor phase epitaxy (HVPE) [4]. The n^{++} Si doping profiles in the GaN emitter and collector are $3 \times 10^{19} \text{ cm}^{-3}$, $5 \times 10^{19} \text{ cm}^{-3}$, respectively (Figure 1c). The substrates have low dislocation densities of approximately 10^6 cm^{-2} . The substrate wafers were cleaned using an aggressive wet chemical etch prior to loading in the ultrahigh vacuum MBE system. Once loaded, the wafers were de-gassed for 30 min at 600 °C and transferred into the MBE deposition chamber. The device layers were grown continuously without interrupts at a constant temperature and growth rate of $\approx 3 \text{ nm/min}$. Transmission electron microscopy (TEM) images confirmed the heterostructures had high crystalline quality [4]. And the hetero-interfaces between GaN and AlN layers were abrupt, ideal for quantum transport devices.

The GaN/AlN heterostructure devices were fabricated using a 5-level mask set that consisted of the following steps: (i) top contact/mesa definition, (ii) bottom contact definition, (iii) device isolation, (iv) via hole creation, and (v) RF pad definition [5]. Both the top and bottom ohmic contacts were a Ti/Al/Ni/Au stack. The isolation was done with a patterned PECVD-SiO₂ top layer, and the via holes were dry-etched with a CF₄ plasma.

All temperature measurements were conducted using a state-of-the-art Lakeshore CPX-HF cryogenic probe station. The system has two 3-axis translation stages built inside its vacuum chamber. One stage was mounted with a ground-signal-ground (GSG) probe with a 200-micron pitch, which could contact devices under test. Bias voltages were applied to the probe via a coaxial cable from outside the chamber. The other stage carried an optical fiber probe. Photon emission was collected by the fiber probe, guided and coupled into a StellarNet UV-VIS spectrometer located outside the chamber via a multimode fiber. The fiber probe had a fixed zenith angle of 30 degree relative to the vertical (z) axis perpendicular to the horizontal plane where the devices were placed. The integration time of the UV spectrometer and the number of scans for averaging were set the same for all the

measurements. The resolution was maintained at 0.5 nm, corresponding to 4.4 meV for wavelength (λ) = 360 nm.

Once a targeted temperature was reached using a computerized thermal feedback loop from a Lakeshore controller, a device under test was contacted by the GSG. The fiber probe was maneuvered to the proximity of the device. Alignment was achieved by reaching spectroscopic maximum at $\lambda \sim 360$ nm. For each temperature, spectra were taken with the device biased at multiple voltages from a source meter located outside the vacuum chamber. Therefore, neither the GSG nor fiber alignment was disturbed during the voltage-dependence studies. However, for temperature-dependence studies, the GSG was lifted up, and then put down for contacting the device again to accommodate possible lateral changes of the GSG probe in response to temperature variations. Alignment between the fiber probe and the device had to be re-done.

3. Results

Figure 2a plots an I-V curve for a GaN/AlN RTD device tested at room temperature ($T = 300$ K). Negative differential resistance (NDR) with a chair-like self-oscillation-related pattern is displayed in the range of 7.0–7.5 V, which confirms the high quality of the PAMBE-grown GaN/AlN heterostructure. The peak-to-valley ratio (PVCR) of the NDR is estimated to be ~ 1.1 , small but acceptable for this research. Figure 2b plots the I-V curves at eight different temperatures ranging from 4.2 to 300 K, showing only slight variations. The bias voltages V_b were limited to the range of 5–6 volts for the unipolar emission characterization. We observed that the UV spectrometer begun to pick up reliable signals once the device under test was biased greater than a threshold of $V_{b,th} \approx 5.0$ V, happening to all the temperatures.

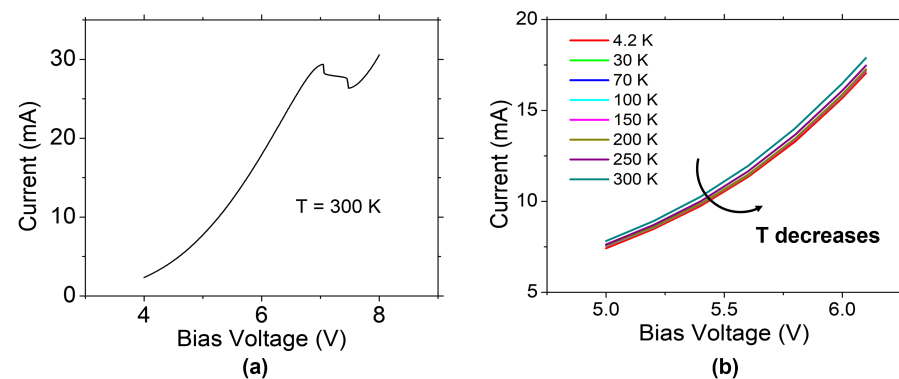


Figure 2. (a) I-V curve at room temperature, and (b) I-V curves at different temperatures.

Figure 3a–e show spectral intensity $\Phi(\lambda)$ vs wavelength (λ) under four different biases: 5.2, 5.4, 5.6 and 5.8 volts at five temperatures: $T = 4.2$ K, 30 K, 70 K, 250 K and 300 K, respectively.

By integrating the spectral intensities over wavelengths numerically, we can estimate light emission power (defined as I), which is presumably proportional to the hole density generated by interband tunneling. We discretized the integral $I = \int d\lambda \Phi(\lambda)$ into the following summation $I \approx \Delta\lambda \sum_k^N \Phi(\lambda_k)$, where $\Delta\lambda = 0.5$ nm is the resolution of UV spectrometer and N is the total number of sampling points. We carried out self-consistent Poisson-Schrödinger calculations showing that the electric field F_{GaN} in the depleted GaN collector—responsible for the interband tunneling—is approximately proportional to the bias voltage V_b (Figure 1d). Because of this linearity, we plot and examine $\ln(I/V_b^2)$ vs. $(1/V_b)$ in Figure 3f, where good linear relationship is exhibited at almost all the temperatures except $T = 4.2$ K. Overall, these fitting curves are consistent with the multiband interband tunneling process described by the Kane model in [6].

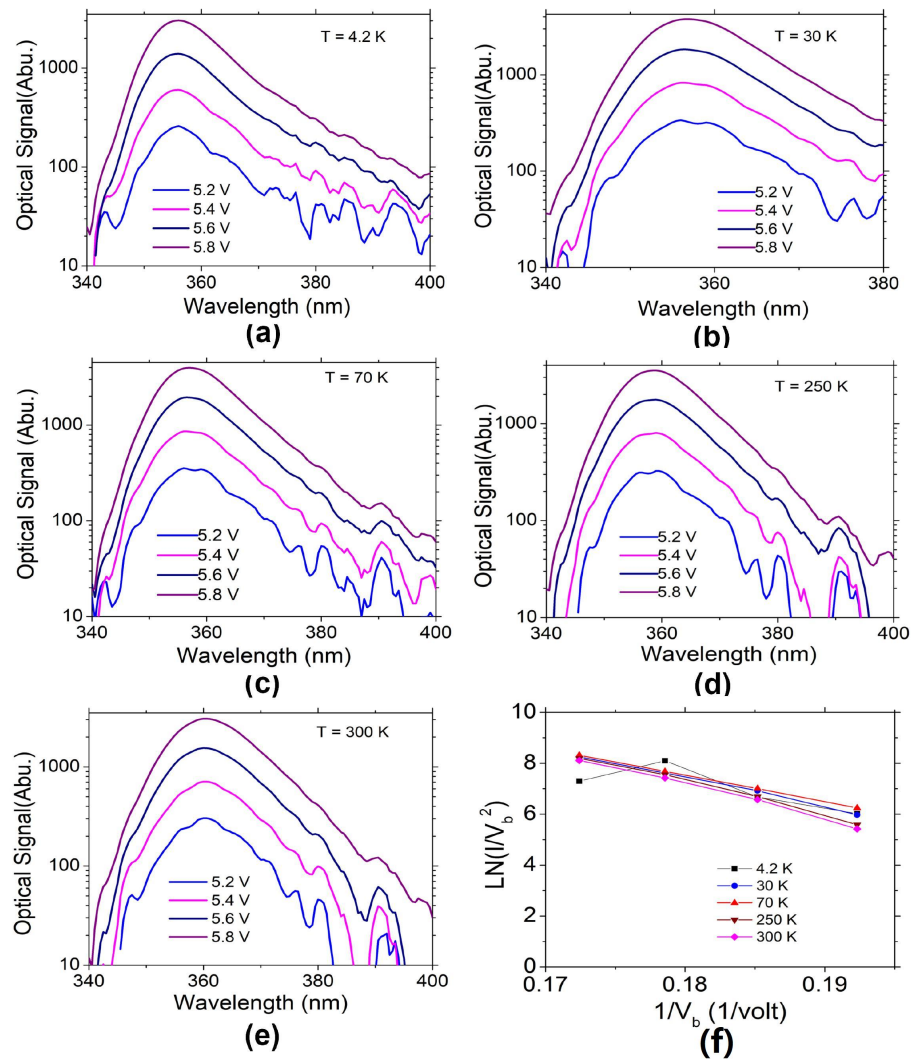


Figure 3. EL spectra at (a) 4.2 K (b) 30 K (c) 70 K, (d) 250 K, (e) 300 K, and (f) $\ln(I/V_b^2)$ vs. $1/V_b$.

Figure 4a plots spectra at $T = 4.2, 30, 70, 250,$ and 300 K, all under the same bias, $V_b = 5.8$ V. Obviously, the peak positions λ_p shifts as the temperature varies. The change of peak emissions, $\Phi(\lambda_p)$, is not monotonic because of the maximum light emission intensity I at $T = 30$ K (Figure 4b). This is inconsistent with the Kane-model prediction that the interband tunneling probability decreases with increasing bandgap, which is monotonically increased by the reduced temperature. However, we should be aware of possible uncertainties in collecting the maximum light emission because the fiber probe was re-aligned with the device every time the temperature was set at a new value.

In the following, we focus on the shifts of peak positions λ_p of Figure 4a. The photon energy $E_{Gp} = hc/\lambda_p$ (h , Planck constant; c , light speed) vs temperature T is plotted in Figure 4c. Similar results are obtained in the rest sets of bias voltages, hence not plotted here. We notice the photon–energy curve bares a strong similarity to the A-exciton-temperature-dependence curve shown in the literature such as [7].

Quantitatively, the bandgap (unit: eV) of bulk GaN vs. temperature is estimated with a formula given by Monemar [8]

$$E_G(T) = 3.503 - 5.08 \times 10^{-4} \frac{T^2}{996K - T} \quad (1)$$

The curve is shown in Figure 4c. The Varshni formula for GaN gives almost the same estimation as the Monemar curve does (Figure 4c) [9,10].

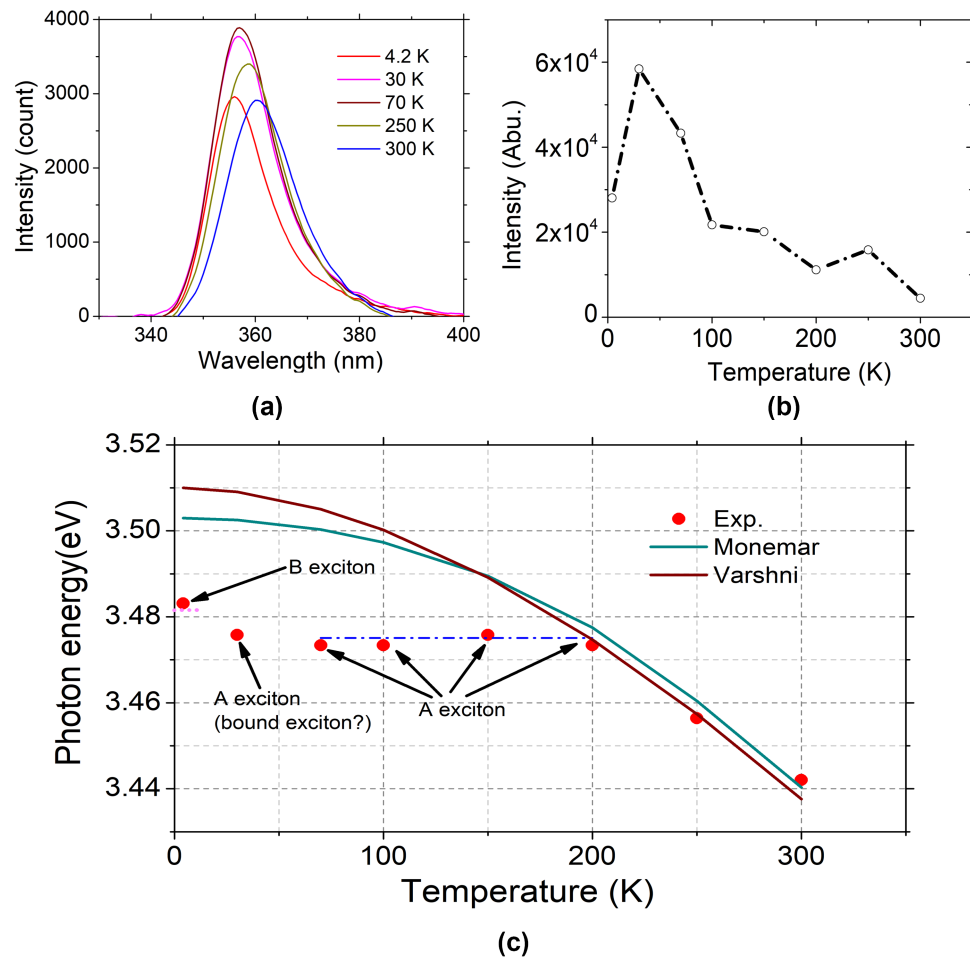


Figure 4. (a) EL spectra at different temperatures, $V_b = 5.8$ V. (b) Light emission vs. temperature. (c) The comparison between the extracted photon energies and the models.

In the range of 200 K–300 K (equivalent to $k_B T = 17.3$ meV to 25.9 meV), the extracted E_{Gp} increases as the temperature drops, and is almost perfectly overlapped with the extrapolated related to experimental bandgap of the bulk GaN. The agreement supports that the unipolar EL is a cross-bandgap (or band-to-band) radiative recombination in the GaN emitter region. It does not come from any impurities. Below $T \sim 200$ K, the experimental peak position E_{Gp} becomes significantly less than the bulk bandgap. Interestingly, the E_{Gp} is almost flat between 30 K and 200 K, but starts to increase again at $T = 4.2$ K.

Exciton in GaN is extensively studied and well understood [7,8,11–18]. We mark the energies of A-exciton transition $A = 3.4751$ eV and (free) B-exciton transition $B = 3.4815$ eV in Figure 4c, respectively [8]. The exciton energies may be slightly changed subject to differences in substrates (e.g., GaN, or sapphire) and strain tensors of structures (e.g., homoepitaxy or heteroepitaxy) [7]. For example, Ref. [7] gives $A = 3.478$ eV, $B = 3.483$ eV; Ref. [15] and Ref. [16] give $A = 3.4776$ eV, $B = 3.4827$ eV; Ref. [17] gives $A = 3.477$ eV, $B = 3.482$ eV; and Ref. [18] gives $A = 3.474$ eV, $B = 3.483$ eV.

By comparing the spectra and extracted peak photon energies with the literature, we categorize the unipolar emission as A-exciton and B-exciton, respectively. The optical transition at ~ 4.2 K is most likely B-exciton emission, being associated with the interband transition Γ_7^V (upper valence band) $\rightarrow \Gamma_7^C$ in bulk GaN. At $T = 30$ K, the emission is likely A-exciton emission but it may be mixed with or even dominated by shallow-donor-bound

exciton emission as the temperature is below ≈ 50 K according to [7,19–23]. Differentiation of the two, free or shallow-donor-bound, requires reflection experiments as only the free (or A type) excitons is strong in reflectance (e.g., [14–16,22]), this is beyond the scope of this paper and may not be feasible for the electroluminescence phenomenon we are investigating. The optical transition in the range of 70 K to 200 K is most likely free A-exciton emission, which is related to the interband transition $\Gamma_9^V \rightarrow \Gamma_7^C$ in GaN.

Figure 5a plots linewidth (or equivalent energy ΔE) vs temperature over three bias voltages, and Figure 5b plots their averages and standard deviations showing similar patterns as the peak position $E_{G,p}$ in Figure 4c. Specifically, the linewidth is the narrowest ≈ 13.0 nm at the lowest 4.2 K. It increases slowly in the range of 30 K–200 K, but starts to increase quickly as the temperature rises above $T = 200$ K. It is estimated to be ≈ 15.8 nm at room temperature, and its equivalent energy is $\Delta E \approx 150.2$ meV which is significantly greater than the thermal broadening $1.8 k_B T \approx 46.6$ meV [24] (k_B , Boltzmann constant). The discrepancy may be explained with the broadening due to random impurity concentration fluctuation, which is estimated ≈ 100 meV according to Ref. [24] because of the heavy doping density in the emitter $3 \times 10^{19} \text{ cm}^{-3}$ (Figure 1c). This impurity broadening from the random distribution of dopants may also be dominant in the spectral linewidth for $T = 4.2$ K.

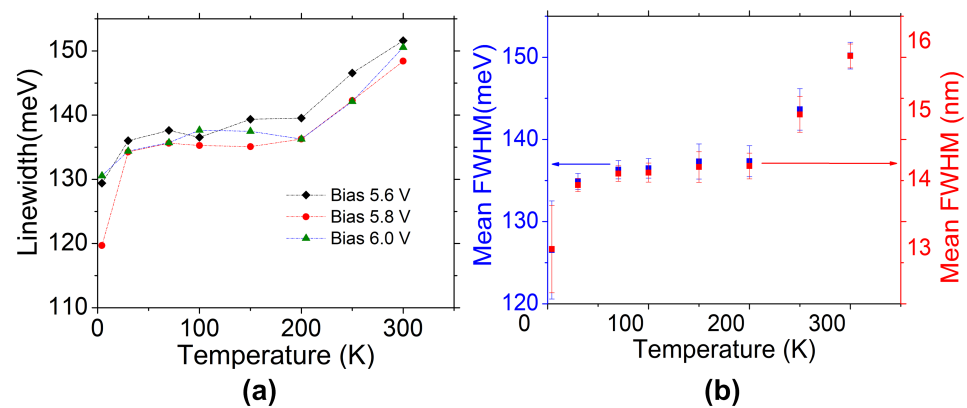


Figure 5. (a) Linewidth vs. temperature curves when bias voltages were 5.6 V, 5.8 V, and 6.0 V. (b) The mean linewidth curves of (a) in the form of both wavelength (right axis) and equivalent energy (left axis).

4. Conclusions

We carried out temperature studies on the EL phenomenon in n-type GaN/AlN heterostructures. At high temperatures 200–300 K, the photon energies and the bulk bandgap of GaN are in close agreement with each other. In the range of 50–200 K, the emission is A-exciton emission, which may be replaced by shallow-donor-bound exciton when the temperature drops below 50 K. At 4.2 K, the EL may transform into B-exciton emission. This confirms the EL is a cross-bandgap electron-hole recombination in GaN, not from any impurities or extrinsic. Without any p-type contacts, the holes are likely produced by the interband tunneling due to the strong polarization fields in Wurtzite heterostructures. The fine spectral features of the excitonic emission were not fully resolved likely because of the limitation from the resolution of the UV spectrometer. This will be pursued in future studies.

Author Contributions: GaN/AlN heterostructure growth, D.F.S. and D.J.M.; device fabrication, T.A.G. and P.R.B.; cryogenic measurement, W.Z. and T.A.G.; formal analysis, W.Z.; T.A.G. and E.R.B.; writing—original draft preparation, W.Z.; writing—review and editing, W.Z., T.A.G., E.R.B. and P.R.B.; funding acquisition, E.R.B. and P.R.B. All authors have read and agreed to the published version of the manuscript.

Funding: This work was performed under the sponsorship of a Multi-University-Research-Initiative (MURI), “Devices and Architectures for THz Electronics (DATE)”—managed by Dr. Paul Maki. This work was supported by the Office of Naval Research and the Under Secretary of Defense for Research and Engineering. We acknowledge the National Science Foundation for support under Grants #1711733 & #1711738.

Institutional Review Board Statement: This research did not involve any humans or animals.

Informed Consent Statement: This research did not involve any humans or animals.

Data Availability Statement: The raw data files for this paper are available upon reasonable request.

Acknowledgments: We thank D. Dauton of Lake Shore Cryotronics for helping use the cryogenics equipment and take some experimental data presented in this paper.

Conflicts of Interest: The authors declare no conflict of interest.

Abbreviations

The following abbreviations are used in this manuscript:

EL	Electroluminescence
MBE	Molecular-beam epitaxy
PAMBE	Plasma-assisted molecular-beam epitaxy
HVPE	Hydride vapor phase epitaxy
PECVD	Plasma Enhanced Chemical Vapor Deposition

References

1. Growden, T.; Zhang, W.-D.; Brown, E.R.; Storm, D.; Meyer, D.; Berger, P. Near-UV Electroluminescence in Unipolar-Doped, Bipolar-Tunneling (UDBT) GaN/AlN Heterostructures. *Nat. Light. Sci. Appl.* **2018**, *7*, 17150. [[CrossRef](#)]
2. Ambacher, O.; Foutz, B.; Smart, J.; Shealy, J.; Weimann, N.; Chu, K.; Murphy, M.; Sierakowski, A.; Schaff, W.; Eastman, L.; et al. Two dimensional electron gases induced by spontaneous and piezoelectric polarization in undoped and doped AlGaIn/GaN heterostructures. *J. Appl. Phys.* **2000**, *87*, 334–344. [[CrossRef](#)]
3. Chow, T.P.; Ghezzi, K. III-Nitride, SiC, and Diamond Materials for Electronic Devices. *Mater. Res. Soc. Symp. Proc.* **1996**, *423*, 69–73.
4. Storm, D.; Growden, T.; Zhang, W.-D.; Brown, E.R.; Nepal, N.; Katzer, D.; Hardy, M.; Berger, P.; Meyer, D. AlN/GaN/AlN resonant tunneling diodes grown by rf-plasma assisted molecular beam epitaxy on freestanding GaN. *J. Vac. Sci. Tech. B* **2017**, *35*, 02B110. [[CrossRef](#)]
5. Growden, T.; Storm, D.; Zhang, W.-D.; Brown, E.R.; Meyer, D.; Fakhimi, P.; Berger, P. Highly repeatable room temperature negative differential resistance in AlN/GaN resonant tunneling diodes grown by molecular beam epitaxy. *Appl. Phys. Lett.* **2016**, *109*, 083504. [[CrossRef](#)]
6. Kane, E. O. Zener tunneling in semiconductors. *J. Phys. Chem. Solids* **1959**, *12*, 181–188. [[CrossRef](#)]
7. Monemar, B.; Bergman, J.; Buyanova, I.; Li, W.; Amano, H.; Akasaki, I. Free Excitons in GaN. *MRS Internet J. Nitride Semicond. Res.* **1996**, *1*, E2. [[CrossRef](#)]
8. Monemar, B. Fundamental energy gap of GaN from photoluminescence excitation spectra. *Phys. Rev. B* **1974**, *10*, 676–681. [[CrossRef](#)]
9. Varshni, Y. Temperature Dependence of the Energy Gap in Semi-Conductor. *Physica* **1967**, *34*, 149–154. [[CrossRef](#)]
10. Eliseev, P. G.; Perlin, P.; Lee, J.; Osiński, M. “Blue” temperature-induced shift and band-tail emission in InGaIn-based light sources. *Appl. Phys. Lett.* **1997**, *71*, 569–571. [[CrossRef](#)]
11. Dingle, R.; Sell, D.D.; Stokowski, S.E. Absorption, Reflectance and Luminescence of GaN Epitaxial layers. *Phys. Rev. B* **1971**, *4*, 1211–1218. [[CrossRef](#)]
12. Monemar, B.; Bergman, J.P.; Amano, H.; Akasaki, I.; Detchprohm, T.; Hiramatsu, K.; Sawaki, N. *Proc International Symposium on Blue Laser and Light Emitting Diodes*; Yoshikawa, A., Kishino, K., Kobayashi, M., Yasuda, T., Eds.; Ohmsha Ltd.: Tokyo, Japan, 1996; pp. 135–140.
13. Eckey, L.; Podlowski, L.; Göldner, A.; Hoffmann, A.; Broser, I.; Meyer, B.K.; Volm, D.; Streibl, T.; Hiramatsu, K.; Detchprohm, T.; et al. Excitonic structure of GaN epitaxial films grown by hydride-vapor-phase epitaxy. *Inst. Phys. Conf. Ser.* **1996**, *142*, 943–946.
14. Stepniewski, R.; Korona, K.P.; Wyszynski, A.; Baranowski, J.M.; Pakula, K.; Potemski, M.; Martinez, G.; Grzegory, I.; Porowski, S. Polariton effects in reflectance and emission spectra of homoepitaxial GaN. *Phys. Rev. B* **1997**, *56*, 15151–15156. [[CrossRef](#)]
15. Pakula, K.; Wyszynski, A.; Korona, K.P.; Baranowski, J.M.; Stepniewski, R.; Grzegory, I.; Bockowski, M.; Jun, J.; Krukowski, S.; Wroblewski, M.; et al. Luminescence and reflectivity in the exciton region of homoepitaxial GaN layers grown on GaN substrates. *Sol. St. Comm.* **1996**, *97*, 919–922. [[CrossRef](#)]

16. Korona, K. P.; Wysmol, A.; Pakula, K.; Stepniewski, R.; Baranowski, J. M.; Grzegory, I.; Lucznik B.; Wróblewski, M.; Porowski, S. Exciton region reflectance of homoepitaxial GaN layers. *Appl. Phys. Lett.* **1996**, *69*, 788–790. [[CrossRef](#)]
17. Kudrawisec, R.; Rudziński, M.; Serafinczuk, J.; Zajac, M.; Misiewicz, J. Photoreflectance study of exciton energies and linewidths for homoepitaxial and heteroepitaxial GaN layers. *J. Appl. Phys.* **2009**, *105*, 093541. [[CrossRef](#)]
18. Bouzidi, M.; Benzarti, A.; Halidou, I.; Chine, Z.; Bchetnia, A.; El Jani, B. Photoreflectance study of GaN grown on SiN treated sapphire substrate by MOVPE. *Superlattices Microstruct.* **2015**, *84*, 13–23. [[CrossRef](#)]
19. Eckey, L.; Holst, J.; Maxim, P.; Heitz, R.; Hoffmann, A.; Broser, I.; Meyer, B.; Wetzel, C.; Mokhov, E.; Baranov, P. Dynamics of bound-exciton luminescences from epitaxial GaN. *Appl. Phys. Lett.* **1996**, *68*, 415–417. [[CrossRef](#)]
20. Smith, M.; Chen, G.D.; Li, J.Z.; Lin, J.Y.; Jiang, H.X.; Salvador, A.; Kim, W.K.; Aktas, O.; Botchkarev, A.; Morkoc, H. Excitonic recombination in GaN grown by molecular beam epitaxy. *Appl. Phys. Lett.* **1995**, *67*, 3387–3389. [[CrossRef](#)]
21. Smith, M.; Chen, G.D.; Lin, J.Y.; Jiang, H.X.; Asif Khan, M.; Sun, C.J.; Chen, Q.; Yang, J.W. Free excitonic transitions in GaN, grown by metal-organic chemical-vapor deposition. *J. Appl. Phys.* **1996**, *79*, 7001–7004. [[CrossRef](#)]
22. Reynolds, D.C.; Look, D.C.; Kim, W.; Aktas, O.; Botchkarev, A.; Salvador, A.; Morkoc, H.; Talwar, D.N. Ground and Excited State Exciton Spectra from GaN Grown by Molecular-Beam Epitaxy. *J. Appl. Phys.* **1996**, *80*, 594–596. [[CrossRef](#)]
23. Kimura, T.; Kataoka, K.; Uedono, A.; Amano, H.; and Nakamura, D. Growth of high-quality GaN by halogen-free vapor phase epitaxy. *Appl. Phys. Express* **2020**, *13*, 085509. [[CrossRef](#)]
24. Schubert, E.F.; Goepfert, I.D.; Grieshaber W. Optical properties of Si-doped GaN. *Appl. Phys. Lett.* **1997**, *71*, 921–923. [[CrossRef](#)]